NASA Technical Memorandum 79127

(NASA-TM-79127) ON THE EQUIVALENCE BETWEEN SEMIEMPIRICAL FRACTURE ANALYSES AND R-CURVES (NASA) 34 p HC A03/MF A01 CSCL 20D

N79-20338

Unclas

G3/34 17069

ON THE EQUIVALENCE BETWEEN SEMIEMPIRICAL FRACTURE ANALYSES AND R-CURVES

Thomas W. Orange
Lewis Research Center
Cleveland, Ohio

TECHNICAL PAPER to be presented at the
Twelfth National Symposium on Fracture Mechanics
sponsored by the American Society for Testing and Materials
St. Louis, Missouri, May 21-23, 1979

INTRODUCTION

This paper examines the relationships between several semiempirical fracture analyses and the R-curve concept of fracture mechanics. These relationships may explain why a semiempirical fracture analysis will yield good results with one set of data and poor results with another. They may also indicate which analyses deserve further consideration.

Over the past decade a number of semiempirical fracture analyses have been presented (refs. 1-5). These analyses all attempt to correlate failure stresses for precracked tension specimens with initial crack length over a range of crack lengths. The correlations involve the determination of one (refs. 1-3) or two (refs. 4,5) empirical parameters from test data. The parameters are treated as material properties which are independent of the specimen and crack configuration but which are functions of specimen thickness and such variables as heat treatment and test temperature. The analyses do not always provide good correlations using data sets other than those chosen by the original authors. To date these analyses have only been formulated for and applied to test specimen configurations. Thus their applicability to the design of complex structural configurations is uncertain.

The progressive development of the R-curve concept has been reviewed in ref. 6. The concept postulates that, for a given material and thickness, there is a unique relationship between the amount of stable crack growth under rising load and the crack-tip stress intensity factor. This relationship is called the crack-extension resistance curve, or R-curve, and represents the response of the material in the vicinity of the crack tip to externally imposed loading. If the R-curve is known, both failure load and critical crack length can be predicted (as functions of initial crack length) for any specimen or structural configuration for which an appropriate stress intensity analysis is available. Thus the R-curve concept appears to be a more useful method than any of the semiempirical analyses.

If the R-curve for a given material and thickness is available, one can calculate fracture stress as a function of original crack length for any test specimen configuration. The converse should also be true. That is, if a relationship between fracture stress and original crack length is available, one should be able to calculate the corresponding R-curve. This observation was the impetus for the present study, which was undertaken to test the following hypotheses:

1) For each semiempirical fracture analysis (SEFA) there is an equivalent R-curve (ERC) whose magnitude and shape are determined by the SEFA formulation and its empirical parameters. The ERC is equivalent in that it predicts exactly the same relationship between fracture stress and original crack length as the SEFA.

2) A SEFA will correlate residual strength data (fracture stress against original crack length) closely if its ERC closely matches the actual R-curve of the material in question, and will correlate poorly if the match is poor.

This paper first reviews some characteristics of the R-curve concept when applied to finite-width specimens. Next the conditions for equivalence between a semiempirical analysis and an R-curve are derived. A hypothetical material is employed to study the relationship between R-curves and semiempirical analyses. Finally, equivalent R-curves are developed for real materials using data from the literature.

SYMBOLS

a	Length of single-tip crack or half-length of double-tip crack, equals $a_o + \Delta$
E'	Effective modulus, equals E for plane stress or $E/(1-\nu^2)$ for plane strain, where E is Young's modulus and ν is Poisson's ratio
G_A	Strain energy release rate
G_R	Crack extension resistance
G_c	Strain energy release rate or crack extension resistance at instability
K_I	Opening-mode stress intensity factor
n	Number of crack tips (one or two)
W	Specimen width
Y	Stress intensity calibration factor, $K_I/\sigma\sqrt{a}$, a dimensionless function of λ
α	Sensitivity factor, eq. (1)
Δ	Effective crack extension (sum of physical crack extension plus a plastic zone correction)
λ	Relative crack length, na/W
σ	Stress normal to crack
σ_u	Ultimate tensile strength
σ_{ys}	Yield strength

Subscripts:

c	at critical or instability condition
o	original value prior to loading

R-CURVE CONCEPT

The R-curve concept and its historical development are reviewed in ref. 6. A general representation of the concept is shown in figure 1a. The strain energy release rate is given by the expression

$$G_A = Y^2\sigma^2 a/E'$$

and represents the driving force (per unit thickness) tending to cause crack propagation. The material's resistance to crack propagation, G_R, is a function of crack extension, Δ. At the critical stress σ_c the driving force curve and the R-curve are tangent. Beyond the point of tangency the driving force increases faster with crack length than does the material's resistance. This instability condition represents the failure of the body.

The point of tangency defines the fracture toughness, G_c , and the critical crack length, $2a_c$. For an infinite body, Y is a constant and the driving force curve is a straight line Thus both the fracture toughness, G_c , and the amount of crack extension at instability, Δ_c , increase with increasing original crack length.

For cracks in simple finite bodies and test specimens, the trends are somewhat different. If we define a dimensionless sensitivity factor as

$$\alpha \equiv \frac{\lambda}{Y}\frac{dY}{d\lambda} \tag{1}$$

then the crack driving force curve and its slope (for constant stress) are

$$E'G_A = Y^2\sigma^2 a$$

$$E'\frac{dG_A}{da} = Y^2\sigma^2(1 + 2\alpha)$$

For convenience, the crack extension resistance curve and its slope are written here as

$$g(\Delta) \equiv E'G_R$$

$$g'(\Delta) \equiv E'\, dG_R/d\Delta$$

At the instability point, $G_A = G_R$ and $dG_A/da = dG_R/d\Delta$ (see figure 1a). If $g(\Delta)$ and $g'(\Delta)$ are mathematically describable, the instability point is determined by the simultaneous solution of two equations,

$$E'G_c = Y_c^2\,\sigma_c^2\,(a_o + \Delta_c) = g(\Delta_c) \tag{2}$$

$$E'\frac{dG_A}{da}\bigg|_{a_c} = Y_c^2\,\sigma_c^2\,(1 + 2\alpha_c) \equiv g'(\Delta_c) \tag{3}$$

The coefficients Y and α are usually expressed as trigonometric or polynomial functions of the relative crack length λ . As a result, a closed-form simultaneous solution is seldom possible, and numerical methods must be used to solve for Δ_c. Then $G_c = g(\Delta_c)/E'$ and the fracture stress σ_c is determined from eq. (2).

As the initial crack length is increased from zero, both G_c and Δ_c increase. However, due to the fact that $dY/d\lambda$ continually increases with λ, both G_c and Δ_c reach maximum values which depend on the specimen width, W, and the forms of both the driving force curve and the R-curve. As a_o is increased still further, both G_c and Δ_c begin to decrease. This behavior is shown schematically in figure 1b where instability curves are shown for a wide range of initial crack lengths. The locus of all instability points is shown by the dotted line. From figure 1b it is also apparent that there are pairs of original crack lengths, say $(a_o)_1 = 0.2\ W$ and $(a_o)_2 \approx 0.7\ W$, which will have the same critical crack extension, $(\Delta_c)_{1,2}$, and fracture toughness, $(G_c)_{1,2}$. From equation (2), the fracture stresses for these original crack lengths are related by

$$\frac{(\sigma_c)_2}{(\sigma_c)_1} = \frac{(Y_c)_1}{(Y_c)_2}\sqrt{\frac{(a_o)_1 + (\Delta_c)_{1,2}}{(a_o)_2 + (\Delta_c)_{1,2}}}$$

Thus there is a relationship between fracture stresses for short cracks and long cracks which is implicit in the R-curve concept, and this relationship is a function of the specimen type and the shape of the R-curve.

It should be noted that, in this paper, Δ is the effective crack extension. It is the sum of the physical crack extension plus an adjustment to account for the effect of crack-tip plasticity.

EQUIVALENCY ANALYSIS

In the preceding section it was shown that, if a mathematical formulation of the R-curve is available, fracture stress can be determined as a function of original crack length. In this section it will be shown that, if an equation for fracture stress as a function of original crack length is available, the equivalent R-curve can be determined. In this paper, only the case where specimen width W is constant is considered. Parallel derivations for the cases where a_o is constant and where a_o/W is constant are given in ref. 7, which contains a more complete treatment of this same subject.

Differentiating both sides of eq. (2) with respect to Δ_c ,

$$\frac{d}{d\Delta_c} EG_c = Y_c^2 \sigma_c^2 \cdot 2\alpha_c \left[\frac{da_o}{d\Delta_c} + 1\right] + Y_c^2 (a_o+\Delta_c) \frac{d}{d\Delta_c} (\sigma_c)^2 + $$
$$+ Y_c^2 \sigma_c^2 \left[\frac{da_o}{d\Delta_c} + 1\right] = g'(\Delta_c)$$

and substituting eq. (3), results in

$$0 = \sigma_c^2 \left[(1+2\alpha_c)\frac{da_o}{d\Delta_c}\right] + (a_o+\Delta_c)\frac{d}{d\Delta_c}(\sigma_c^2) \qquad (4)$$

Assume that there is a function f such that we can define

$$\left.\begin{aligned} f(a_o) &\equiv \sigma_c^2 \\ f'(a_o) &\equiv d(\sigma_c^2)/da_o \end{aligned}\right\} \text{for } W = \text{constant}$$

Then eq. (4) becomes

$$0 = \frac{da_o}{d\Delta_c}\left[(1 + 2\alpha_c) f(a_o) + (a_o + \Delta_c) f'(a_o)\right]$$

and since $da_o/d\Delta_c \neq 0$ we have

$$0 = (1 + 2\alpha_c) f(a_o) + (a_o + \Delta_c) f'(a_o) \qquad (5)$$

For cracks in infinite bodies, $\alpha = 0$ and eq. (5) becomes

$$\Delta_c = \frac{f(a_o)}{-f'(a_o)} - a_o \tag{6}$$

which, after substituting the infinite-body formulations for $f(a_o)$ and $f'(a_o)$ from the APPENDIX, gives Δ_c for any a_o in terms of the empirical parameters. Then terms can be rearranged to give a_o as a function of Δ_c, say

$$a_o = F(\Delta_c)$$

Substituting this function into eq. (2) yields

$$E'G_c = Y_c^2 \left[F(\Delta_c) + \Delta_c\right] \cdot f\left[F(\Delta_c)\right] \tag{7}$$

Since eq. (6) gives Δ_c for any value of a_o, eq. (7) must give $E'G_c$ for any and all values of Δ_c, which is a definition of the R-curve. Thus, after writing the function F in terms of the empirical parameters, it is appropriate to write eq. (7) in the general terms of $E'G_R$ and Δ, rather than $E'G_c$ and Δ_c. The end result is an explicit ERC formulation in terms of the empirical parameters.

To determine the ERC for cracks in finite bodies, an indirect method is required. First, the finite-body formulations for $f(a_o)$ and $f'(a_o)$ from the APPENDIX are substituted into eq. (5). Because of the more complicated nature of the finite-body formulations, it is unlikely that an explicit function $F(\Delta_c)$ will be obtainable. But for any given value of Δ_c, a_o is a root of eq. (5) which may be found by standard numerical methods and which represents a single value of $F(\Delta_c)$. Substituting this value into eq. (7) yields a discrete point on the ERC. By incrementing Δ_c and repeating the calculation, the ERC can be determined point by point.

ANALYTICAL COMPARISONS

Dimensionless Equivalent R-Curves

It is helpful and more efficient to first compare semiempirical fracture analyses (SEFA) and equivalent R-curves (ERC) on an analytical basis. This is most easily done using the problem of a crack in an infinite plate as a baseline.

The infinite-body ERC for Kuhn's analysis (ref. 1) is obtained using the method described in the paragraph containing eqns. (6) and (7). Substituting eqns. (A1) and (A2) from the APPENDIX into eqns. (6) and (7) with $Y_c^2 = \pi$ yields

$$\Delta_c = \sqrt{a_o} / C_m \tag{8a}$$

$$E'G_R = \frac{\pi \sigma_u^2 \Delta}{1 + C_m^2 \Delta} \tag{9a}$$

where C_m is an empirical parameter having units $(L^{-\frac{1}{2}})$. Equation (9a) is plotted in dimensionless form in figure 2a. This curve obviously resembles an R-curve and might be expected to closely match some (but not all) experimental R-curves.

The infinite-body ERC for Orange's analysis (ref. 2) is obtained in the same manner. Using eqns. (A3) and (A4) results in

$$\Delta_c = (K_u / \sigma_u)^2 / \pi \tag{8b}$$

$$E'G_R = K_u^2 \tag{9b}$$

where K_u is an empirical parameter having units $(FL^{-3/2})$. These equations define a single point. In order to relate this single point to the R-curve concept, the point may be thought of as the corner of a step-function, and that step-function might in turn be considered as a very simple approximation of an actual R-curve.

The infinite-body ERC for Feddersen's analysis (ref. 3) is obtained by substituting eqns. (A5) and (A6) into eqns. (6) and (7) as before, yielding

$$\Delta_c = \frac{27}{8\pi}\left(\frac{K_c}{\sigma_{ys}}\right)^2 - \frac{3}{2}a_o \qquad (8c)$$

$$E'G_R = K_c^2\left\{1 + \left[\frac{4\pi}{9}\left(\frac{\sigma_{ys}}{K_c}\right)^2\Delta\right] + \frac{1}{3}\left[\frac{4\pi}{9}\left(\frac{\sigma_{ys}}{K_c}\right)^2\Delta\right]^2 + \frac{1}{27}\left[\frac{4\pi}{9}\left(\frac{\sigma_{ys}}{K_c}\right)^2\Delta\right]^3\right\} \qquad (9c)$$

for $a_o \le (9/4\pi)(K_c/\sigma_{ys})^2$ where K_c is an empirical parameter having units $(FL^{-3/2})$. Equation (8c) requires that critical crack extension decrease as original crack length increases from zero. This is in direct opposition to the R-curve concept and is not supported by any data known to this author. Equation (9c), which is plotted in figure 2b, does not look at all like an R-curve but does satisfy the requirements of coincidence and tangency. For $a_o = 0$, the point of tangency is the right-hand terminus of the curve. As a_o increases, the point of tangency moves downward and leftward along the curve. Finally, at $a_o = (9/4\pi)(K_c/\sigma_{ys})^2$, the point of tangency is the left-hand terminus.

The infinite-body ERC for Newman's analysis (ref. 4) is obtained by substituting eqns. (A11) and (A12) into eqns. (6) and (7) as before, yielding

$$\Delta_c = \frac{m\,K_f}{\sigma_u}\sqrt{\frac{a_o}{\pi}} \qquad (8d)$$

$$E'G_R = \frac{\sigma_u^2\Delta}{m^2/\pi + (\sigma_u/K_f)^2\Delta} \qquad (9d)$$

where K_f is an empirical parameter having units $(FL^{-3/2})$ and m is a dimensionless empirical coefficient which is not greater than unity. Equation (9d) is plotted in dimensionless form in figure 2c. This ERC is asymptotic to $E'G_R = K_f^2$, and the coefficient m determines the rapidity of the approach. As m decreases from unity to near-zero, the ERC develops a progressively sharper knee. The flexibility of this two-parameter ERC should allow it to match R-curves for a wide range of real materials.

The infinite-body ERC for Bockrath's analysis (ref. 5) is obtained by substituting eqns. (A13) and (A14) into eqns. (6) and (7) as before, resulting in

$$\Delta_c = (\omega/2)a_o \quad (8e)$$

$$E'G_R = \frac{\pi}{2}(2 + \omega)K_{Tc}^{2}\left(\frac{2}{\omega}\Delta\right)^{\frac{\omega}{2+\omega}} \quad (9e)$$

where ω is a dimensionless empirical coefficient and K_{Tc} is an empirical parameter having irrational units (FL^{ω}). Equation (9c) is plotted in figure 2d. This ERC has no asymptote, and its slope is infinite at $\Delta=0$. Except for notation, it is identical to the R-curve model proposed by Broek as equation (10) of ref. (8). Broek's model was derived using R-curve concepts and the experimental observation that, for small cracks in wide specimens, the critical crack length is often proportional to the initial crack length.

At this point we can state the following. For each SEFA, in its infinite-body form at least, there is indeed an ERC. For four of the analyses considered, the ERC resembles or approximates an actual R-curve. The ERC for Feddersen's analysis does not resemble an R-curve and will not be considered further.

Comparisons Using Synthetic Data

Hypothesis (2) of the INTRODUCTION postulates that a SEFA will correlate residual strength data closely if its ERC closely matches the actual R-curve and will correlate poorly if the match is poor. To test this hypothesis we would need, as a minimum, both residual strength data (for several specimen sizes having a wide range of crack lengths) and R-curve data for two materials having significantly different R-curve shapes. Since no such body of data is known to this author, it was necessary to synthesize one. This was done by formulating two R-curve equations using the following guidelines. First, to avoid exact fits, neither equation should be mathematically equivalent to one of the ERC formulations previously derived. Second, one R-curve should have a definite knee, the other should be gently curving. Using these equations, synthetic test data can be generated by instability analysis for any specimen size and type. An advantage of this approach is the total absence of data scatter.

Unobtainium is assumed to be a heat-treatable material. Since the material is imaginary, the units will be left to the reader's imagination. In the annealed condition, its ultimate tensile strength is 150 and its R-curve is given by

$$E'G_R = 8{,}000\sqrt{10\Delta - \Delta^2} \qquad (10a)$$

In the aged condition, its ultimate tensile strength is 200 and its R-curve is given by

$$E'G_R = \frac{50{,}000}{\pi}\arctan(10\Delta) \qquad (10b)$$

These are shown in figure 3. The coefficients in eqns. (10) were selected so that the significant features of both curves would lie within the ranges $0 \le E'G_R \le 25{,}000$ and $0 \le \Delta \le 1$.

The pseudotest data points are calculated using conventional instability analysis as follows. Dividing eq. (2) by eq. (3) and rearranging terms gives

$$0 = \frac{g(\Delta_c)}{g'(\Delta_c)} - \frac{a_o + \Delta_c}{1 + 2\alpha_c} \qquad (11)$$

The functions $g(\Delta_c)$ and $g'(\Delta_c)$ are given by one of eqns. (10) and its derivative. The factor α_c is determined using eq. (1) and the secant stress intensity calibration factor for uniformly-loaded center-crack specimens (ref. 9). Then, for prescribed values of a_o and W, Δ_c is the least positive root of eq. (11). This root can be found by any of several numerical methods. Next, Δ_c is substituted back into eq. (10) to calculate $E'G_c$. Finally, the fracture stress σ_c is obtained from eq. (2).

The "specimens" that are studied here were sized as follows. For the infinite-width pseudotests, the initial crack half-lengths a_o were chosen (by trial and error) to give Δ_c values well distributed over the entire R-curve. For the finite-width pseudotests, the specimen widths were fixed at 8 times (first series) and 4 times (second series) the largest initial crack half-length in the infinite-width series. The calculated values of stress and crack extension at instability are given in Table I. The values of stress and initial crack length were then used as inputs to the various semiempirical analyses.

The empirical parameters were determined as follows. Kuhn's parameter C_m was calculated for each specimen in the infinite-width series using eq. (A1). The simple average of seven values, $\overline{C}_m$, is given in Table I. The bar is used here to denote the average value for one data set. Orange's parameter, K_u, was also calculated for each specimen in the infinite-width series using eq. (A3). The average value $\overline{K}_u$ given in Table I is a weighted average determined in the same manner as eq. (6) of ref. 2. Newman's parameters $\overline{K}_F$ and $\overline{m}$ were determined using the least-squares procedure given in Appendix C of ref. 4. Bockrath's parameters $\overline{K}_{Tc}$ and $\overline{\omega}$ were determined by a least-squares fit of eq. (A13). Since Bockrath's method is restricted to cases where the crack area is less than 10 percent of the gross area, specimens having $a_o > W/20$ were excluded from the least-squares fit.

The equivalent R-curves were calculated as follows. For the infinite-width series, the empirical parameters from Table I were simply substituted into the appropriate one of eqns. (9). For the finite-width series, the indirect method (described in the paragraph containing eq. (7)) was used. Specifically, eqns. (A9) and (A10) or eqns. (A13) and (A14) were used along with eqns. (5) and (7) and the appropriate empirical parameters.

The residual strength of the infinite-width Unobtainium is shown in figure 4. For the annealed condition, Bockrath's semiempirical fracture analysis (SEFA) provides a nearly perfect fit to the pseudodata. When ranked according to the sum of the squares of deviations, Newman's SEFA, Kuhn's, and Orange's follow in that order. For the aged condition, the ranking is quite different. Here Newman's SEFA provides a nearly perfect fit, with Orange's, Kuhn's, and Bockrath's following in that order. The equivalent R-curves (ERC) are shown in figure 5. For the annealed condition, The Bockrath ERC matches the actual R-curve almost perfectly. When ranked according to the integral of the square of the deviation, the Newman ERC, the Kuhn ERC, and the Orange ERC follow in that order. For the aged condition, the Newman ERC is the best match to the actual R-curve. The Bockrath ERC, the Kuhn ERC, and the Orange ERC follow in that order. The Orange ERC, although crude, is a better approximation for the aged material than for the annealed.

Since the Orange ERC is rather crude and since Kuhn's SEFA is equivalent to a special case of Newman's (see APPENDIX, following eq. (A12)), these two were not considered further. The Newman and Bockrath ERCs for finite-width center-crack series are shown in figures 6 and 7. Here the same trends are seen as in the infinite-width series. The Bockrath ERC is the better match for the annealed condition, while the Newman ERC is the better match for the aged condition. Note in Table I that the empirical parameters $\overline{K}_{Tc}$, $\overline{\omega}$, $\overline{K}_f$, and $\overline{m}$ all vary slightly with specimen width. The ERCs shown in figures 5-7 are also distinctly different for different specimen widths, but the differences are slight.

The results of this exercise using synthetic data can be summarized as follows. Hypothesis (2) of the INTRODUCTION postulates that an SEFA will correlate residual strength data closely if its ERC closely matches the actual R-curve and will correlate poorly if the match is poor. Strictly speaking, this hypothesis cannot be proven, since the ERC magnitude and shape depend on empirical parameters which must be obtained from residual strength data. However, the converse appears to be true. That is, if a SEFA correlates residual strength data closely, its ERC will closely match the actual R-curve. Furthermore it is apparent that if, for a given material and thickness, the R-curve is unique the various empirical parameters are not, and vice versa.

COMPARISONS USING ACTUAL TEST DATA

As mentioned earlier, experimental studies containing both residual strength and actual R-curve data are relatively few in number. Nevertheless, enough were found in the literature to allow some comparisons to be made using actual data obtained from real materials.

NASA Data for 2014-T6 Aluminum Alloy

In reference 10 this author presented test data for 2014-T6 aluminum alloy specimens 1.5 mm (0.06 in) thick, tested at 77 K (-320°F). Figure 14 of that reference presented typical curves of crack growth against applied stress for notches of six initial lengths in 30-cm (12-in) wide specimens. Those curves were developed by plotting individual crack growth data points for replicate specimens, then drawing a smooth curve to give a good visual average. For the present report, those data were re-analyzed. The crack extension resistance and effective crack length were computed for each data point as

$$E'G_R = \sigma^2 \pi a_{eff} \text{ secant}(\pi a_{eff}/W)$$

$$a_{eff} = a + (E'G_R/2\pi\sigma_{ys}^2)$$

respectively. Since these equations are transcendental, an iterative solution was required. A total of 176 data points were obtained from 17 specimens with initial crack lengths ($2a_o$) ranging from 3 mm to 100 mm (1/8 to 4 in). The empirical parameters for the Newman and Bockrath SEFAs were determined in the manner described earlier. As before, only specimens with $a_o \leq W/20$ were included in the Bockrath analysis. The fitted empirical parameters are listed in Table II.

Residual strength is shown in figure 8a. Newman's SEFA gives a good fit over the entire range. Bockrath's SEFA fits the short-crack data fairly well, but the fit would be poor if extrapolated to longer cracks. The R-curve data points and the equivalent R-curves are shown in figure 8b. Both ERCs fit the data rather well, with Bockrath's somewhat better at small crack extensions and Newman's somewhat better for larger extensions. These results suggest that the ERC concept applies to real data as well as to synthesized data.

Boeing Data for 2219-T87 Aluminum Alloy

Earlier it was shown using synthetic data that, if the actual R-curve is unique, one obtains slightly different values of the empirical parameters from data sets for specimens having different widths. Data from the Boeing Co. for 2219-T87 aluminum alloy specimens have the same characteristics. These data originally appeared in an internal report (Eichenberger, T. W.: Fracture Resistance Data Summary, Report D2-20947, Boeing Airplane Co., June 1962), but are also tabulated in reference 1. Center-crack specimens 2.5 mm (0.10 in) thick were tested. The data for specimens 60 and 120 cm (24 and 48 in) wide are used here because they cover a wide range of initial crack lengths.

Bockrath's analysis was not applied since only one of the wider specimens had $a_0 \leq W/20$. Newman's parameters were determined separately for each specimen width, and somewhat different values were obtained as can be seen in Table II. The residual strength curves fit the data quite well, as can be seen in figure 9a, with the average error being less than 3½ percent. Using a method that is outside the scope of this paper, it was found that the actual R-curve for this material could be estimated by

$$E'G_R = 8.07\times10^{15}\,\Delta^{0.554}$$

where $E'G_R$ is in N^2/m^3 and Δ is in cm, or by

$$E'G_R = 11.2\times10^{9}\,\Delta^{0.554}$$

where $E'G_R$ is in lb^2/in^3 and Δ is in inches. Residual strengths calculated from this equation using conventional instability analysis are also shown in figure 9a. The agreement is very slightly better than for Newman's SEFA, the average error being less than 3 percent. The estimated R-curve and the Newman ERCs are shown in figure 9b, and as expected the differences are small. Although these data tend to support the concept of a unique R-curve, the differences are so small as to be within the bounds of probable data scatter.

CONCLUDING REMARKS

The results of this study lead to the following conclusions:

1. - For each semiempirical fracture analysis (SEFA) there is an equivalent R-curve (ERC) whose magnitude and shape are determined by the SEFA formulation and its empirical parameters. The ERC is equivalent in that it predicts exactly the same relationship between fracture stress and initial crack length (residual strength) as the SEFA.

2. - If, for a given set of data, a SEFA correlates residual strength closely, its ERC will closely approximate the effective R-curve of the test material.

3. - Of the five SEFAs examined, Newman's (ref. 4) appears to be the most generally useful. Bockrath's SEFA (ref. 5), which is only formulated for quasi-infinite bodies, is too restrictive for widespread use. Three (refs. 1-3) do not appear to warrant further consideration.

4. - If the effective R-curve is indeed unique, then the various empirical parameters cannot be constant, and vice versa.

The analytical comparisons made herein indicate that the variations in Newman's parameters are small enough that the differences may well be within the range of normal data scatter for real materials. Thus a very carefully planned and conducted experiment would be required to determine which concept (R-curve or SEFA) is more appropriate.

REFERENCES

1. Kuhn, Paul: Strength Calculations for Sheet-Metal Parts with Cracks. Materials Res. & Standards, vol. 8, no. 9, Sept. 1968, pp. 21-26.

2. Orange, Thomas W.: A Semiempirical Fracture Analysis for Small Surface Cracks. Engng. Fracture Mech., vol. 3, no. 1, July 1971, pp. 53-67.

3. Feddersen, C. E.: Evaluation and Prediction of the Residual Strength of Center Cracked Tension Panels. Damage Tolerance in Aircraft Structures, STP-486, ASTM, 1971, pp. 50-78.

4. Newman, J. C., Jr.: Fracture Analysis of Surface- and Through-Cracked Sheets and Plates. Engng. Fracture Mech., vol. 5, no. 3, Sept. 1973, pp. 667-689.

5. Bockrath, G. F., and Glassco, J. B.: A Theory of Ductile Fracture. Report MDC-G2895, McDonnell Douglas Astronautics Co., April 1974.

6. Heyer, R. H.: Crack Growth Resistance Curves (R-Curves) - Literature Review. Fracture Toughness Evaluation by R-Curve Methods, STP-527, ASTM, 1973, pp. 3-16.

7. Orange, Thomas W.: A Relationship Between Semiempirical Fracture Analyses and R-Curves. NASA TP- (in preparation), 1979.

8. Broek, D.: The Effect of Finite Specimen Width on the Residual Strength of Light Alloy Sheet. Report NLR-TR M.2152, National Aerospace Laboratory (Netherlands), Sept. 1965.

9. Feddersen, C. E.: (discussion in) Plane Strain Crack Toughness Testing of High Strength Metallic Materials, STP-410, ASTM, 1966, pp. 77-79.

10. Orange, Thomas W.: Fracture Toughness of Wide 2014-T6 Aluminum Sheet at -320°F. NASA TN D-4017, 1967.

APPENDIX

SEMIEMPIRICAL FRACTURE ANALYSES

P. Kuhn (1968). - Equations (3) and (4) of ref. 1 give the fracture stress for a finite-width center-crack plate. For an infinite plate, these may be rewritten and differentiated as

$$f(a_o) = \sigma_u^2 \left[1 + C_m \sqrt{a_o}\right]^{-2} \quad \text{(A1)}$$

$$f'(a_o) = -f(a_o) \cdot (1 + C_m \sqrt{a_o})^{-1} \cdot C_m / \sqrt{a_o} \quad \text{(A2)}$$

where C_m is an empirical parameter having units $(L^{-1/2})$.

T. Orange (1969). - Equation (8) of ref. 2 gives the fracture stress for a finite-width center-crack plate. For an infinite plate, this reduces to

$$f(a_o) = K_u^2 \left[\pi a_o + (K_u/\sigma_u)^2\right]^{-1} \quad \text{(A3)}$$

$$f'(a_o) = -f(a_o) \left[a_o + K_u^2/\pi\sigma_u^2\right]^{-1} \quad \text{(A4)}$$

where K_u is an empirical fracture toughness parameter having units $(FL^{-3/2})$.

C. Feddersen (1970). - For an infinite plate, eqns. (6) and (10) of ref. 3 reduce to

$$f(a_o) = \sigma_{ys}^2 \left[1 - \frac{4\pi}{27}\left(\frac{\sigma_{ys}}{K_c}\right)^2 a_o\right]^2 \quad \text{(A5)}$$

$$f'(a_o) = -f(a_o) \left[\frac{27}{8\pi}\left(\frac{K_c}{\sigma_{ys}}\right)^2 - \frac{a_o}{2}\right]^{-1} \quad \text{(A6)}$$

for $a_o \leq (9/4\pi)(K_c/\sigma_{ys})^2$ and eq. (7) to

$$f(a_o) = K_c^2/\pi a_o \quad \text{(A7)}$$

$$f'(a_o) = -f(a_o)/a_o \quad \text{(A8)}$$

APPENDIX

SEMIEMPIRICAL FRACTURE ANALYSES

P. Kuhn (1968). - Equations (3) and (4) of ref. 1 give the fracture stress for a finite-width center-crack plate. For an infinite plate, these may be rewritten and differentiated as

$$f(a_o) = \sigma_u^2 \left[1 + C_m \sqrt{a_o}\right]^{-2} \tag{A1}$$

$$f'(a_o) = -f(a_o) \cdot (1 + C_m \sqrt{a_o})^{-1} \cdot C_m/\sqrt{a_o} \tag{A2}$$

where C_m is an empirical parameter having units $(L^{-\frac{1}{2}})$.

T. Orange (1969). - Equation (8) of ref. 2 gives the fracture stress for a finite-width center-crack plate. For an infinite plate, this reduces to

$$f(a_o) = K_u^2 \left[\pi a_o + (K_u/\sigma_u)^2\right]^{-1} \tag{A3}$$

$$f'(a_o) = -f(a_o) \left[a_o + K_u^2/\pi\sigma_u^2\right]^{-1} \tag{A4}$$

where K_u is an empirical fracture toughness parameter having units $(FL^{-3/2})$.

C. Feddersen (1970). - For an infinite plate, eqns. (6) and (10) of ref. 3 reduce to

$$f(a_o) = \sigma_{ys}^2 \left[1 - \frac{4\pi}{27}\left(\frac{\sigma_{ys}}{K_c}\right)^2 a_o\right]^2 \tag{A5}$$

$$f'(a_o) = -f(a_o)\left[\frac{27}{8\pi}\left(\frac{K_c}{\sigma_{ys}}\right)^2 - \frac{a_o}{2}\right]^{-1} \tag{A6}$$

for $a_o \leq (9/4\pi)(K_c/\sigma_{ys})^2$ and eq. (7) to

$$f(a_o) = K_c^2/\pi a_o \tag{A7}$$

$$f'(a_o) = -f(a_o)/a_o \tag{A8}$$

for $a_o \geq (9/4\pi)(K_c/\sigma_{ys})^2$, where σ_{ys} is the material's yield strength and K_c is an empirical fracture toughness parameter.

J. Newman (1972). - Equation (12) of ref. 4 for a finite-width center-crack plate can be rewritten and differentiated as

$$f(a_o) = K_f^2\left[\sqrt{\pi a_o \sec(\pi a_o/W)} + \frac{m}{1-\lambda_o}\frac{K_f}{\sigma_u}\right]^{-2} \quad (A9)$$

$$f'(a_o) = -\frac{f(a_o)}{a_o}\,\frac{\left[1+\frac{\pi a_o}{W}\tan(\frac{\pi a_o}{W})\right]\sqrt{\pi a_o \sec(\frac{\pi a_o}{W})} + \frac{2\lambda_o}{(1-\lambda_o)^2}\frac{mK_f}{\sigma_u}}{\sqrt{\pi a_o \sec(\frac{\pi a_o}{W})} + \frac{1}{1-\lambda_o}\frac{mK_f}{\sigma_u}} \quad (A10)$$

which, for an infinite plate, reduce to

$$f(a_o) = K_f^2\left[\sqrt{\pi a_o} + mK_f/\sigma_u\right]^{-2} \quad (A11)$$

$$f'(a_o) = -f(a_o)\sqrt{\pi/a_o}\left[\sqrt{\pi a_o} + mK_f/\sigma_u\right]^{-1} \quad (A12)$$

where K_f is an empirical fracture toughness parameter and m is a dimensionless empirical coefficient which is not greater than unity. Note that if we let $m=1$ and $K_f = \sigma_u\sqrt{\pi}/C_m$, eq. (A11) reduces to eq. (A1).

G. Bockrath (1972). - Equation (13) of ref. 5 for a center-crack plate is limited to $\lambda_o \leq 0.1$, which approximates an infinite plate. Thus

$$f(a_o) = K_{Tc}^2\,(a_o)^{-\frac{2}{2+\omega}} \quad (A13)$$

$$f'(a_o) = -\frac{2}{2+\omega}f(a_o)/a_o \quad (A14)$$

where ω is a dimensionless empirical coefficient and K_{Tc} is an empirical parameter having irrational units of (FL^{ω}).

TABLE I. - PSEUDOTEST DATA FOR HYPOTHETICAL MATERIAL UNOBTAINIUM AND FITTED EMPIRICAL PARAMETERS

Annealed Condition; σ_u = 150

	W = ∞		W = 8.8		W = 4.4	
a_o	Δ_c	σ_c	Δ_c	σ_c	Δ_c	σ_c
0.10	0.0980	112.56	0.0971	112.42	0.0945	112.00
.21	.2015	93.25	.1939	92.75	.1757	91.36
.32	.3008	83.70	.2773	82.71	.2313	80.08
.44	.4044	77.08	.3529	75.43	.2692	71.29
.56	.5036	72.36	.4137	69.98	.2901	64.26
.80	.6897	65.82	.4996	61.79	.2986	52.84
1.10	.9016	60.36	.5580	54.09	.2713	41.02
$\overline{C}_m$	1.355		NOT COMPUTED			
$\overline{K}_u$	111.8					
$\overline{K}_{Tc}$	62.13		60.76		59.52	
$\overline{\omega}$	1.853		1.727		1.642	
$\overline{K}_f$	165.7		172.8		159.6	
$\overline{m}$	0.8549		0.8497		0.7800	

Aged Condition; σ_u = 200

	W = ∞		W = 96		W = 48	
a_o	Δ_c	σ_c	Δ_c	σ_c	Δ_c	σ_c
0.05	0.0953	162.93	0.0953	162.93	0.0953	162.92
.36	.2014	100.08	.2014	100.07	.2013	100.05
1.0	.3067	69.77	.3064	69.74	.3055	69.64
2.0	.4135	52.91	.4121	52.82	.4081	52.58
3.2	.5093	43.37	.5054	43.21	.4942	42.73
6.4	.6978	31.93	.6791	31.50	.6286	30.21
12.0	.9346	23.95	.8566	22.87	.6760	19.60
$\overline{C}_m$	1.820		NOT COMPUTED			
$\overline{K}_u$	140.7					
$\overline{K}_{Tc}$	63.80		66.57		68.38	
$\overline{\omega}$	0.838		1.151		1.310	
$\overline{K}_f$	163.3		166.0		168.4	
$\overline{m}$	0.7266		0.7378		0.7469	

TABLE II. - EMPIRICAL PARAMETERS FOR TEST DATA FROM THE LITERATURE

Data Source, ref. __	Alloy	Specimen Constant	Empirical Parameters, ref. 4			Empirical Parameters, ref. 5[a]		
			$\overline{K}_f$		$\overline{m}$	$\overline{K}_{Tc}$		$\overline{\omega}$
			$MN\ m^{-3/2}$	ksi $\sqrt{in}$		SI Units	English Units	
10	2014-T6	W = 30 cm	89.9	81.8	0.8094	99.70 $MN\ m^{-1.761}$	34,790 lb $in^{-1.761}$	2.188
1	2219-T87	W = 60 cm	183.1	166.6	.8841	NOT COMPUTED		
		W = 120 cm	210.2	191.3	1.0			

(a) Only specimens having $a_o \leq W/20$ were included in least squares fit.

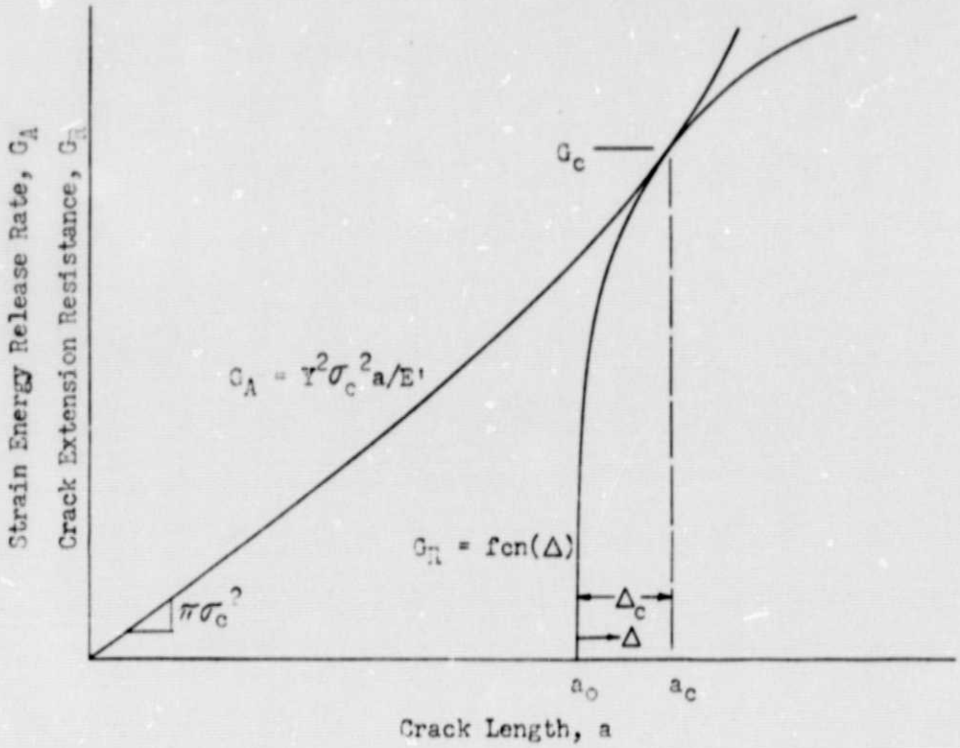

a) General representation of R-curve instability concept.

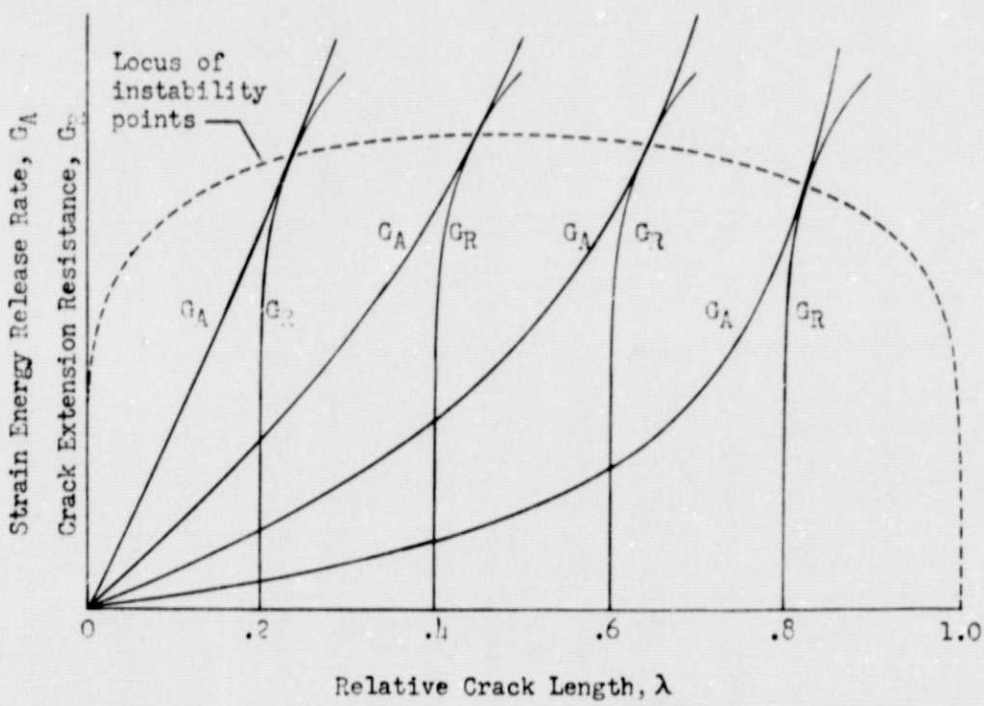

b) R-curve instability for a wide range of initial crack lengths.

Figure 1. - R-curve instability concepts.

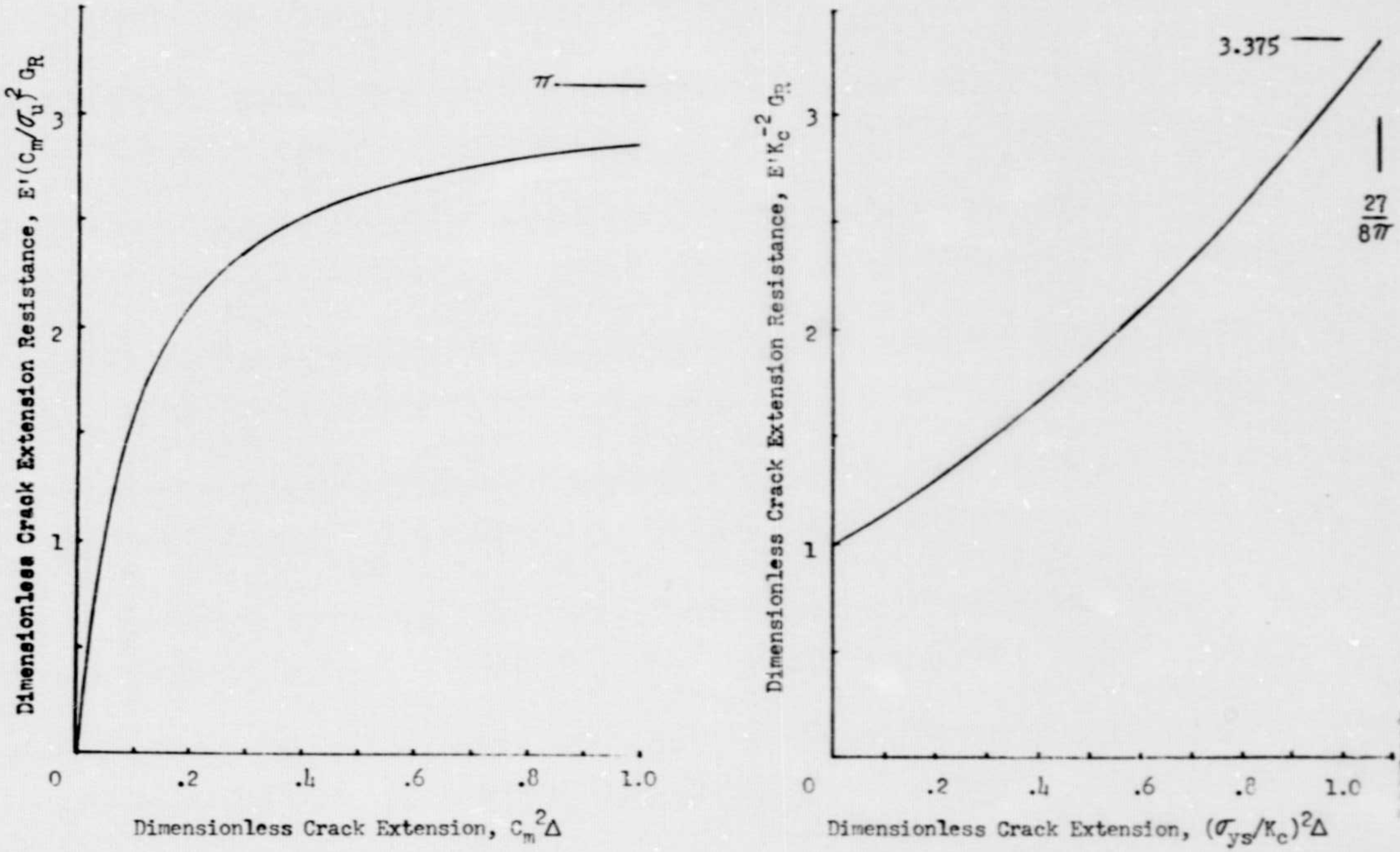

a) Kuhn's analysis (ref. 1).

b) Feddersen's analysis (ref. 3).

Figure 2. - Dimensionless R-curves equivalent to various semiempirical fracture analyses for the case of a crack in an infinite plate.

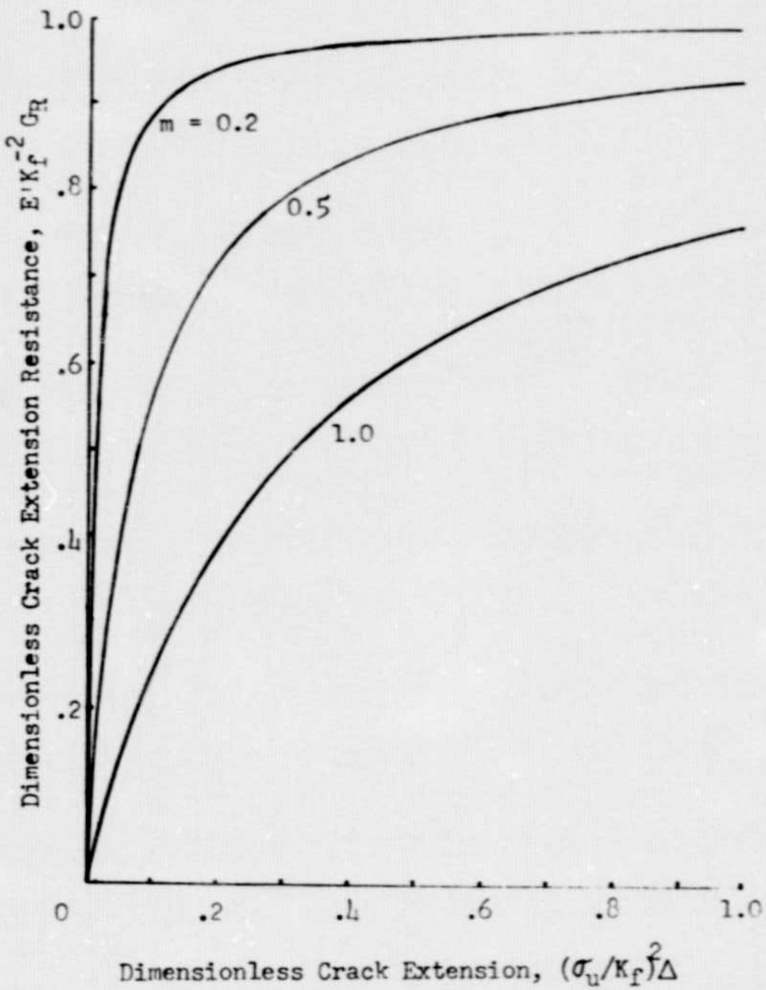

c) Newman's analysis (ref. 4).

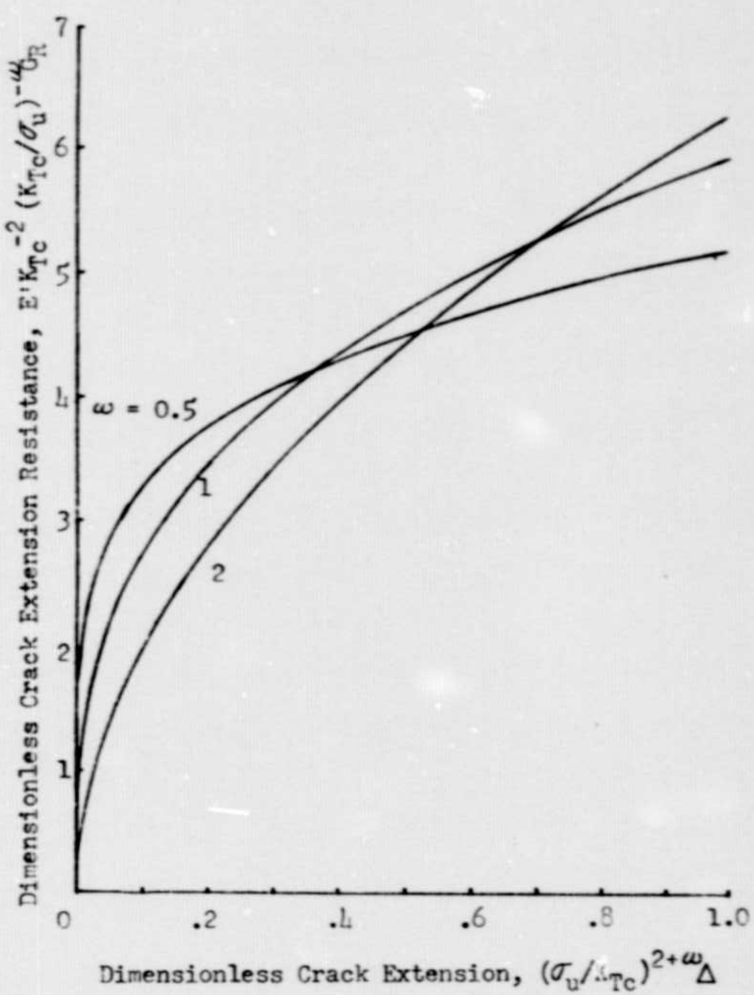

d) Bockrath's analysis (ref. 5).

Figure 2. - continued.

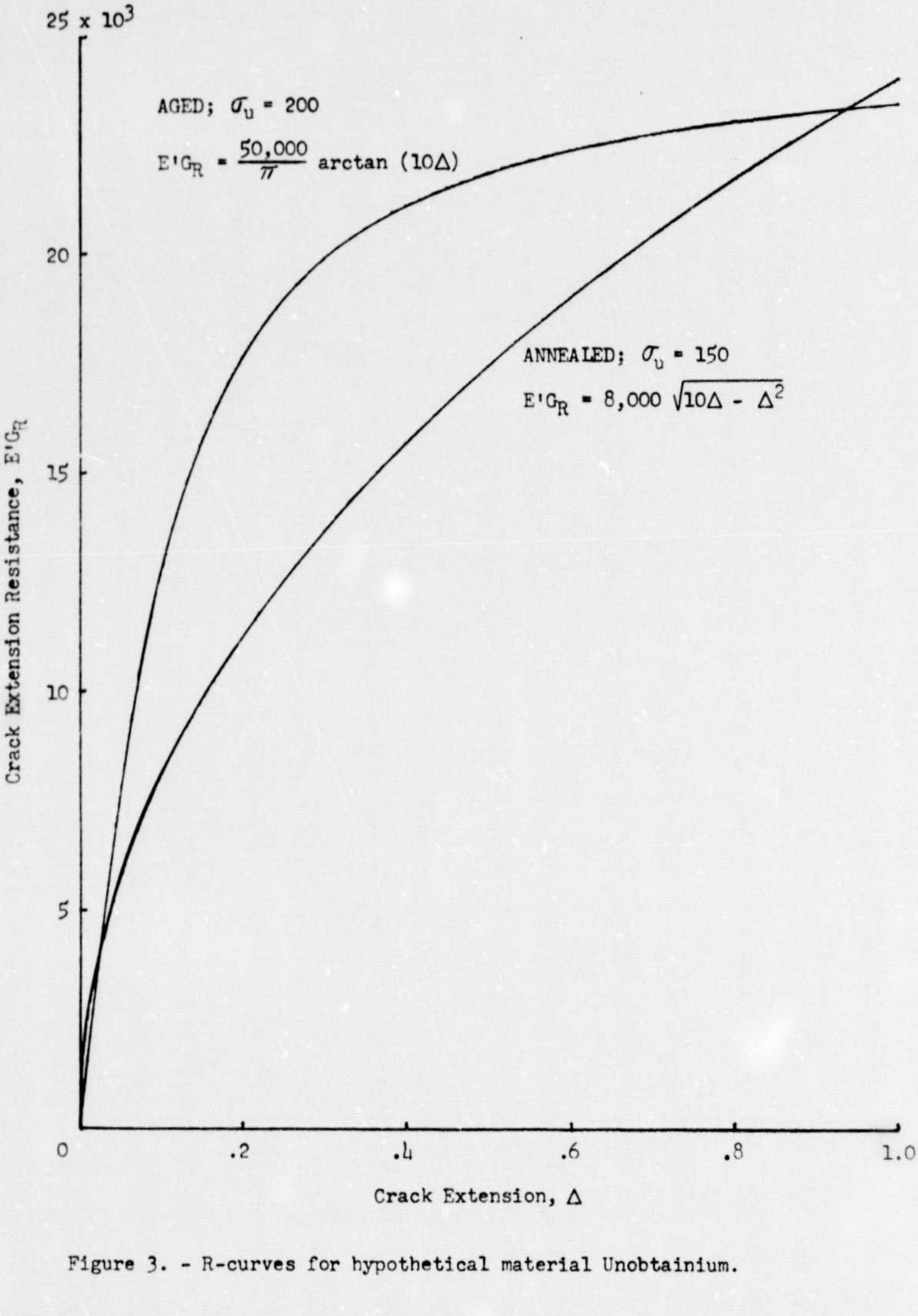

Figure 3. - R-curves for hypothetical material Unobtainium.

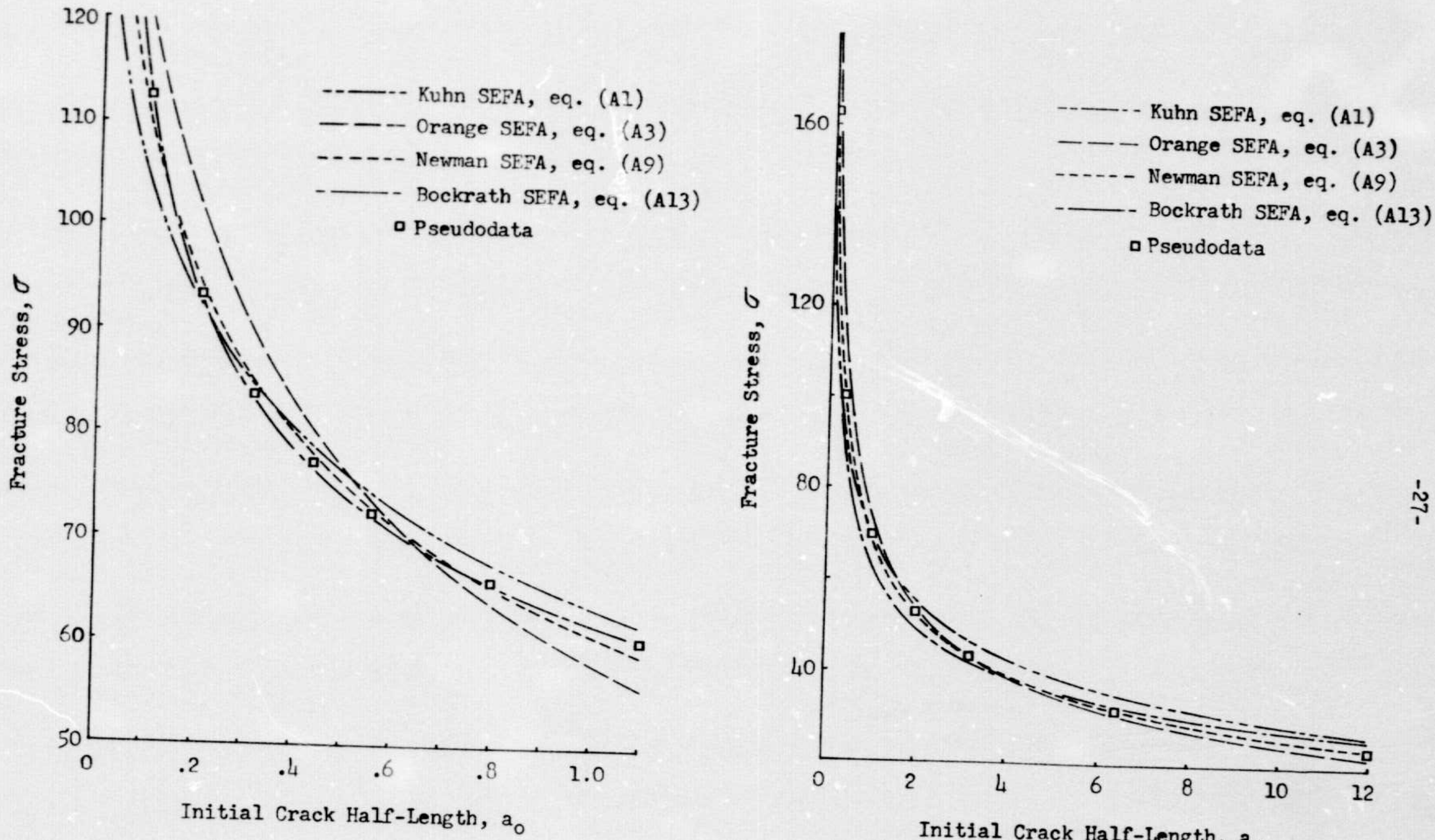

a) Annealed condition, σ_u = 150 .

b) Aged condition, σ_u = 200 .

Figure 4. - Residual strength of hypothetical material Unobtainium, infinite-width series; various semiempirical fracture analyses (SEFA) fit to pseudotest data.

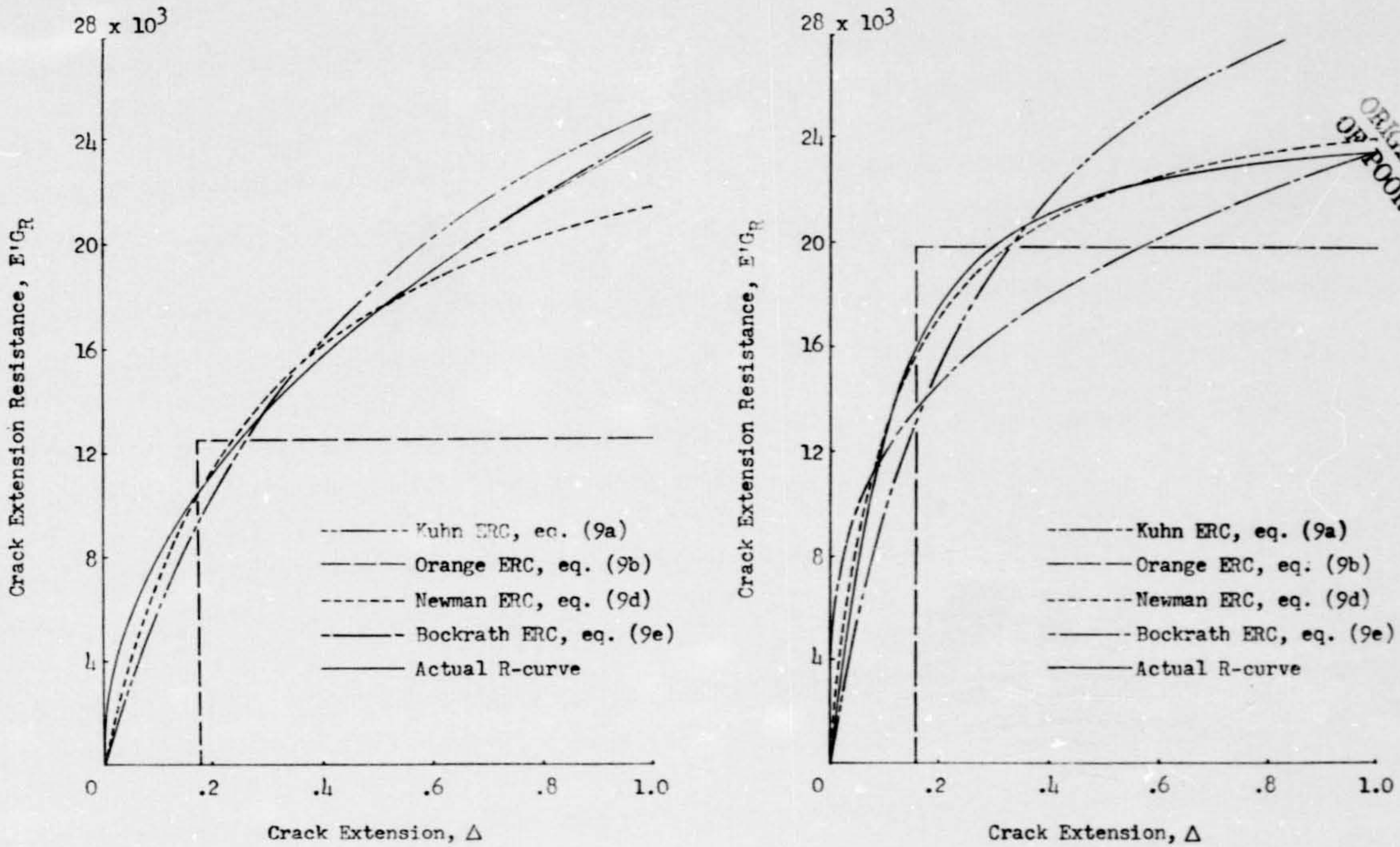

a) Annealed condition.

b) Aged condition.

Figure 5. - Actual R-curves and equivalent R-curves (ERC) for hypothetical material Unobtainium, infinite-width series.

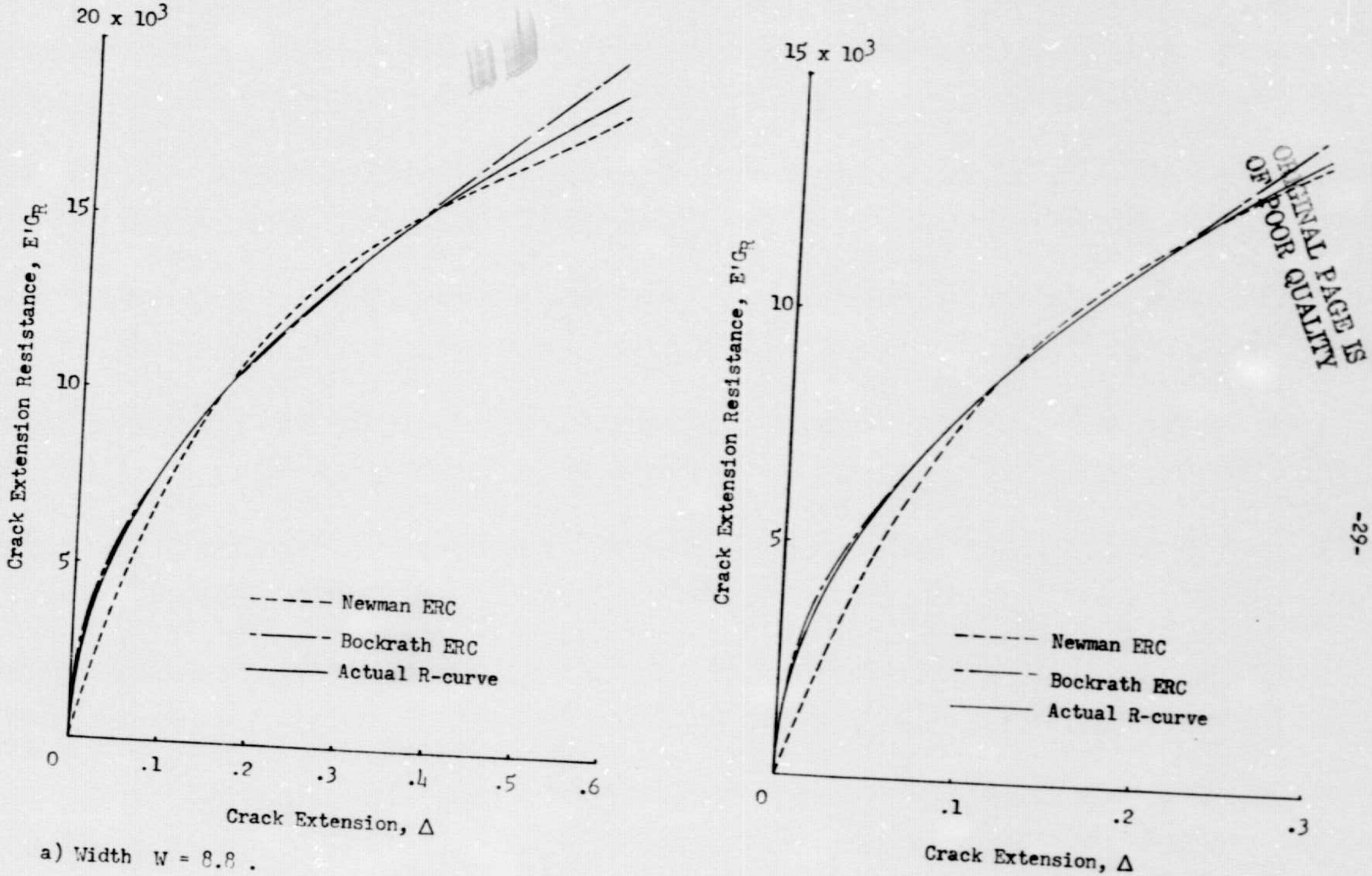

a) Width $W = 8.8$.

b) Width $W = 4.4$.

Figure 6. - Actual R-curve and equivalent R-curves (ERC) for hypothetical material Unobtainium, finite width, annealed condition.

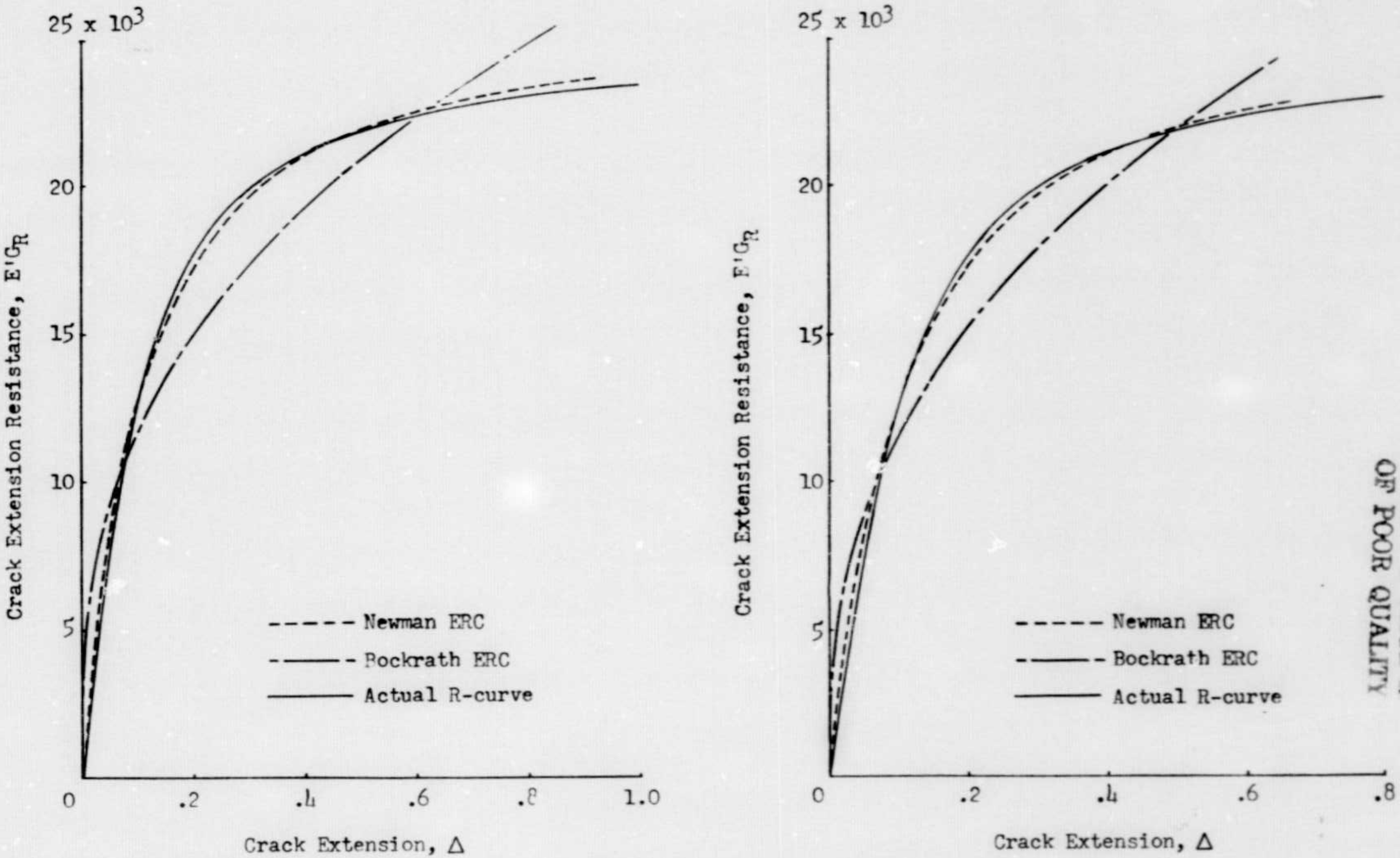

a) Width W = 96 .

b) Width W = 48 .

Figure 7. - Actual R-curve and equivalent R-curves (ERC) for hypothetical material Unobtainium, finite width, aged condition.

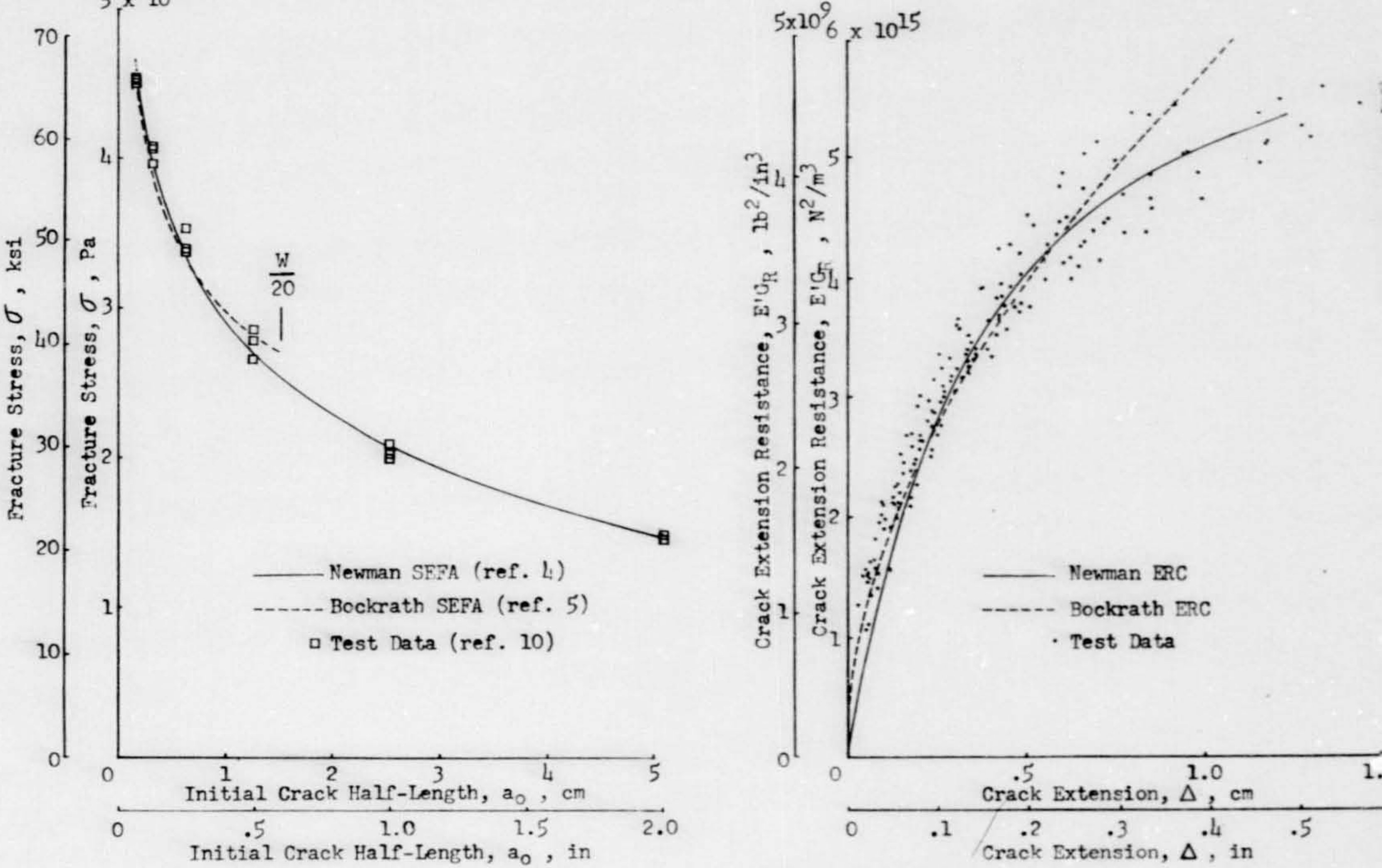

a) Residual Strength

b) Equivalent R-curves (ERC) and test data.

Figure 8. - Residual strength, equivalent R-curves, and R-curve data points for 2014-T6 aluminum alloy sheet at 77 K (ref. 10).

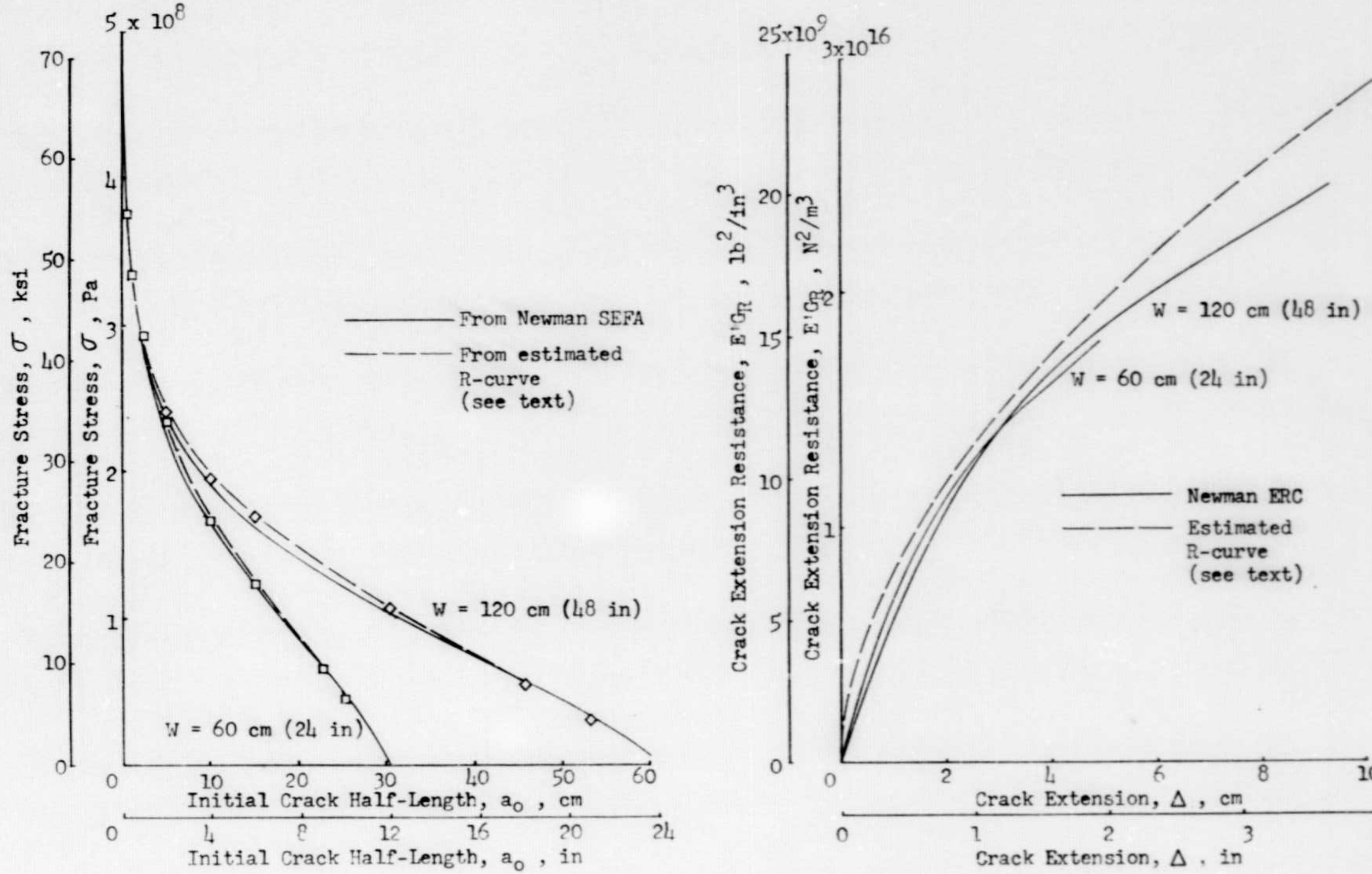

a) Residual strength.

b) Equivalent R-curves (ERC) and estimated R-curve.

Figure 9. - Residual strength, equivalent R-curves, and estimated R-curve for 2219-T87 aluminum alloy sheet (data from ref. 1).